

# A Topological Nomenclature for 3D Shape Analysis in Connectomics

Abhimanyu Talwar, Zudi Lin, Donglai Wei\*, Yuesong Wu, Bowen Zheng,  
Jinglin Zhao, Won-Dong Jang, Xueying Wang, Jeff W. Lichtman, and  
Hanspeter Pfister

Harvard University, Cambridge, MA 02138, USA

**Abstract.** An essential task in nano-scale connectomics is the morphology analysis of neurons and organelles like mitochondria to shed light on their biological properties. However, these biological objects often have tangled parts or complex branching patterns, which makes it hard to abstract, categorize, and manipulate their morphology. Here we propose a topological nomenclature to name these objects like chemical compounds for neuroscience analysis. To this end, we convert the volumetric representation into the topology-preserving reduced graph, develop nomenclature rules for pyramidal neurons and mitochondria from the reduced graph, and learn the feature embedding for shape manipulation. In ablation studies, we show that the proposed reduced graph extraction method yield graphs better in accord with the perception of experts. On 3D shape retrieval and decomposition tasks, we show that the encoded topological nomenclature features achieve better results than state-of-the-art shape descriptors. To advance neuroscience, we will release a 3D mesh dataset of mitochondria and pyramidal neurons reconstructed from a 100 $\mu$ m cube electron microscopy (EM) volume. Code is publicly available at <https://github.com/donglaiw/ibexHelper>.

**Keywords:** Connectomics · Shape Analysis · Nomenclature.

## 1 Introduction

Recent advancement in large-scale electron microscopy (EM) allows generation of terabyte and petabyte of serial images of brain tissue at nanometer resolution [7,18]. Machine learning methods have made automated 3D reconstruction possible for individual neurons [6] and intracellular organelles such as mitochondria [2]. Intriguingly, 3D shapes of these objects resolved at EM level are far more complicated than the classic depiction in the textbook. Thus, novel morphology analysis tools are demanded to further our understanding of the basic properties of neuronal compartments (Fig. 1).

---

\* Email: [donglai@g.harvard.edu](mailto:donglai@g.harvard.edu).

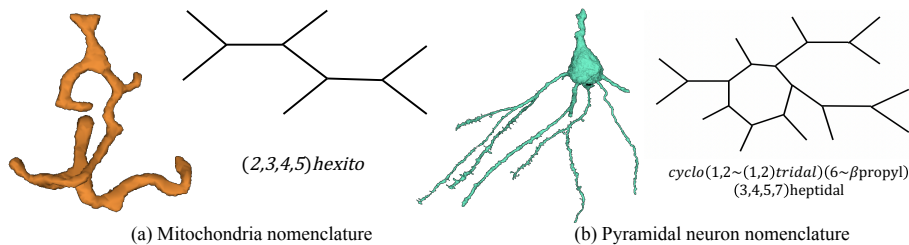


**Fig. 1.** Graph representation and topological nomenclature for mitochondria and pyramidal neurons in EM connectomics. Our proposed algorithm generates reduced graph representation of the 3D meshes for intuitive perception and nomenclature for concise scientific communication.

Nevertheless, there are three challenges. First, the branches and loops of a non-convex object can tangle together in the 3D meshes, which makes it difficult for an intuitive perception of the underlying topology. Second, there lacks an intuitive way to convey the shape information of neurons and organelles in the neuroscience community. Third, traditional descriptors of 3D meshes are designed to compare objects with similar scales, which is not suitable for the application on neurons and organelles that have a wide range of spatial size.

To tackle these challenges, we propose a topological nomenclature system to abstract, categorize, and manipulate the 3D meshes of neurons and organelles. We first skeletonize them into vertexes and edges to untangle the objects, which are further pruned into a concise reduced graph while preserving topological properties. To systematically name those objects, we propose a nomenclature system borrowing ideas from nomenclature for organic compounds. The primary aim of nomenclature in chemistry is to ensure that every name refers to a specific compound without ambiguity. The naming systems, including InChI [5] and SMILES, displays more structural details but is more cumbersome for scientific communication. Therefore in this work, we follow the IUPAC rule [14] to generate the graph name that is more human-readable. To apply the nomenclature system to shape analysis, we use the deep learning model for self-supervised learning on graph [9]. In comparison with traditional shape descriptors like heat kernel signature (HKS) [12], one key difference from our approach is that our graph representations are more intuitive to understand than the HKS and allow for a simple shape decomposition into primitives. The idea of the skeleton based 3D shape matching has been explored by Sundar *et al.* in [17] who introduce the concept of a topological signature vector - a low dimensional representation of a graph which can be used by similarity measures. One difference from our approach is that their scheme generates an acyclic skeletal graph which does not capture cycles or multiple paths between two vertexes.

To summarize, we present three main contributions in this paper. First, we propose a shape abstraction method that converts 3D meshes into 2D graphs to improve morphological perception. Second, by using the nomenclature system, we not only make it more interpretable for neuroscientists but also further

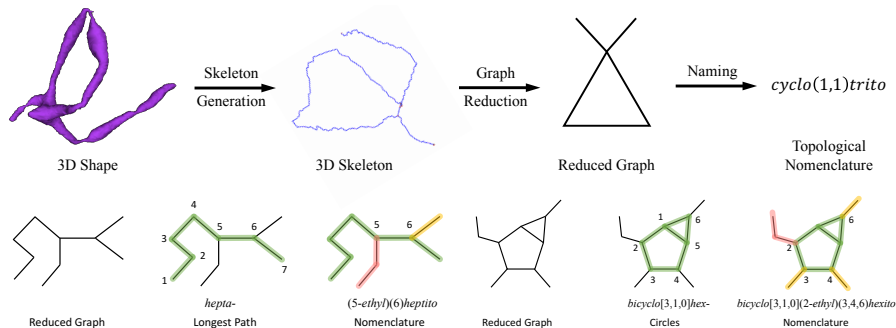


**Fig. 2.** Illustration of our topological nomenclature pipeline (first row) and nomenclature rules (second row). Best view in color.

compress the information needed for graph reconstruction. Third, we implement an unsupervised model to embed these graphs into vector space for 3D shape retrieval and decomposition.

## 2 Method

Given an input 3D mesh, we first transform it into a reduced graph which preserves its topological information, then determines its nomenclature name based on its object type (e.g., mitochondria), and lastly compute its feature in the nomenclature embedding space for later manipulation (Fig. 2).

### 2.1 Topology-Aware Reduced Graph Generation

Starting from the voxel representation of a 3D mesh, we convert it into a reduced graph which preserves its topological structure, like the molecular graph [10].

**Graph Initialization:** We use an off-the-shelf skeletonization algorithm proposed in Kálmán [13] to extract a 3D skeleton from the voxel representation. We can view the extracted 3D skeleton as a weighted undirected graph  $G = (V, E, W)$  where  $V \subset \mathbb{Z}^3$  is the set of coordinates of skeleton nodes in the 3D voxel grid,  $E \subset V \times V$  is the set of edges, and  $W \subset \mathbb{R}^+$  is the set of edge weights.

**Graph Reduction:** Based on the degree of incident edges, we can divide the skeleton vertices  $V$  into junctions  $J = \{n \in V : degree(n) > 2\}$  and endpoints  $E = \{n \in V : degree(n) = 1\}$ . We aim to reduce the skeleton graph  $G$  to a graph  $G_S$  whose set of vertices is  $J \cup E$  (referred to as the *key nodes*), and which preserves topological features of  $G$  such as paths and distances (along with the 3D skeleton) between any pair of key nodes. Further, we also require  $G_S$  to preserve any cycles present in the skeleton graph  $G$  and to preserve multiple paths between any two key nodes.

For graph reduction, we modify the *Breadth-First-Search* traversal algorithm, as outlined in Algorithm 1 in the supplementary material. At each step of the

traversal, we only enqueue key nodes to our traversal queue. We initialize the queue with any key node, and while visiting a key node  $v$ , we only enqueue (1) any key nodes which are adjacent to  $v$ , and (2) any other key nodes which are connected to  $v$  by a path in  $G$  comprising only of non-key nodes (referred to as a *simple path*). We define the “thickness” of an edge as the average of distance transforms of its two vertices, and the “thickness” of a path can be calculated as the mean of the thickness of each edge on the path weighted by edge lengths. During traversal, we keep track of two metrics for every pair of key nodes connected by a simple path: (1) sum of lengths of all edges in  $G$  on that simple path, and (2) mean thickness of that simple path.

**Graph Post-procession:** Often small biological structures do not contribute much to the overall function. To further simplify the graph, we can remove edges and cycles whose path length is small relative to the total length of edges in  $G_S$ . Thus, we collapse all edges with a length lower than a threshold value of  $\tau$ . With bigger  $\tau$ , we obtain a coarser-level representation of the graph.

## 2.2 Topological Nomenclature Rules

Our nomenclature system is modified upon the IUPAC nomenclature of organic chemistry, which is not only invariant to the deformation and the graph indexing order but also easily convertible back to the graph representation. We add suffixes *-ito* and *-idal* to mitochondria and pyramidal neurons respectively.

**Acyclic Graph:** An acyclic graph is a graph having no cycles. A reduce graph can be entirely a tree structure or contain tree branches. The nomenclature rule for a tree is first to count the longest chain of vertexes, and assign a prefix based on the number of vertexes (e.g., the longest chain with  $n = 5$  vertexes has a prefix *penta*). Find the longest path in a general graph has been shown to be a *NP*-complete problem [3], but find the longest path in an undirected tree graph can be solved efficiently by running the breadth-first search (BFS) algorithm twice (see the supplementary material for detail). Therefore the rule makes sure that for acyclic graphs not only computer programs but also human users can efficiently drive the corresponding topological nomenclature. Then every vertex on the longest path is assigned a location number from 1 to  $n$ . For a branch, we use the location index as prefix and name the branch recursively based on the rules. For simplicity, we combine the prefix of branches with the same structure and omit the description for branch topology if a branch only contains one node.

**Cyclic graph:** If the reduced graph has circles, then we assign a higher priority to the circles and name the graph accordingly. For the graph structure with one circle, the prefix is *cyclo*. We then name branches use parentheses containing relative location on the ring together with the branch description described before. For a bicyclic graph where two circles share at least one vertexes, the root numeral prefix of the graph name depends on the total number of vertexes in all rings together[4]. The prefix *bicyclo* denote the sharing of at least two vertexes, while *spiro* denote the sharing of only one vertex. In between the prefix and the suffix, a pair of brackets with numerals denotes the number of vertexes between

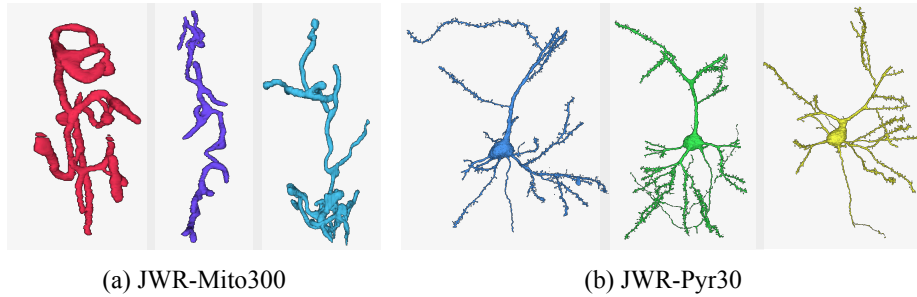


**Fig. 3.** Samples in JWR-Mito300 and JWR-Pyr30 datasets. (a) Unlike textbook illustrations, mitochondria can have complicated 3D shapes. (b) Pyramidal neurons exhibit great diversity in the spatial distribution of dendrites and their branching patterns.

each of the bridgehead ones. These numbers are arranged in descending order and are separated by periods. For example, a graph with a 3-vertex circle and a 5-vertex circle share two vertexes (one edge) will be named *bicyclo*[3, 1, 0]*hexito* (Fig. 2). Such rules can be easily extrapolated into graphs with more than three circles, and we refer the reader for more detail in the supplementary material.

### 2.3 Topological Nomenclature Embedding

We extract features from the graphs to calculate the similarity between them. For graph representation, we construct adjacency matrices of the graphs, whose elements are connectivities between nodes. We employ a variational graph auto-encoder (VGAE) [9] to extract features for each adjacency matrix. VGAE is a neural network for unsupervised learning on graphs based on a variational autoencoder [8]. In VGAE, we first normalize the adjacency matrix using the symmetric normalization scheme. Then, we perform graph convolutions on the normalized adjacency matrix. Finally, VGAE reconstructs the adjacency matrix by adopting a fully connected layer. The network is trained to minimize the difference between the input adjacency matrix and the reconstructed one. We use the output of the graph convolutions for nomenclature embedding.

## 3 Dataset

**Data Acquisition:** We imaged a tissue block from Layer II/III in the primary visual cortex of an adult rat at a resolution of  $4 \times 4 \times 30 \text{ nm}^3$  using a multi-beam scanning electron microscope. After stitching and aligning the 2D images on multi-CPU clusters, we obtained a final 3D image stack of  $100 \mu\text{m}$  cube.

**Object Segmentation:** We adopted the 3D U-Net model [15] for initial automatic neuron segmentation and mitochondria segmentation. Then we used a manual annotation tool [1] to proofread the segmentation results.

**JWR-Mito300:** We reconstructed all the mitochondria found in the somata of 11 cells: one pyramidal neuron, six interneurons, and four glial cells. From all

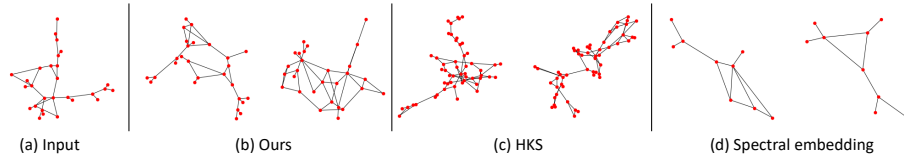


**Fig. 4.** Given (a) input 3D meshes, we show top-2 retrieval results for (b) our topological nomenclature, (c) Heat Kernel Signature (HKS), (d) spectral embedding.

the fully-segmented mitochondria, we selected 316 of them that have nontrivial topological structures with a volumetric size larger than  $0.2 \mu m^3$  (Fig. 3a).

**JWR-Pyr30:** We randomly selected 30 pyramidal cells whose cell bodies are located in the central volume with the presence of a significant portion (if not full) of their basal dendrites. Individual pyramidal neurons have one apical dendrite pointing to the pial surface and an axon often extending in the opposite direction. Nevertheless, they all show distinct distributions of oblique and basal dendrites (Fig. 3b).

## 4 Experiments

In this section, we first evaluate our nomenclature extraction result both quantitatively and qualitatively. Then we show two applications for 3D shape analysis with the extracted nomenclature for mitochondrion and pyramidal neurons. For quantitative evaluation of our nomenclature method, we asked neuroscientists to draw their imagined reduced graph when showing them with the original 3D object meshes. We then count the ratio of ‘correct’ graph based on the perception of experts. We found over 70% of the graphs are identical to the perception of experts. We refer readers for more details in the supplementary material.

### 4.1 3D Shape Retrieval

For a given query 3D shape, users may want to find similar shapes from the entire dataset. To this end, we perform 3D shape retrieval using the proposed topological nomenclature. The goal of this experiment is to find two topological shapes that are similar to the given query 3D shape. For the JWR-Mito300 dataset, we set every 3D shape as a query and discover its two nearest neighbors.

To compare two 3D shapes, we first compute pairwise differences between nomenclature embeddings from different 3D shapes by computing  $L2$  distances. Then, we determine a similarity between the two 3D shapes as a mean of matching costs. We use the Hungarian matching.

Figure 4 shows 3D shape retrieval results of the proposed algorithm compared to both HKS [16] and spectral embedding [11]. The results indicate that the proposed algorithm discovers topologically similar 3D shapes. In contrast, HKS

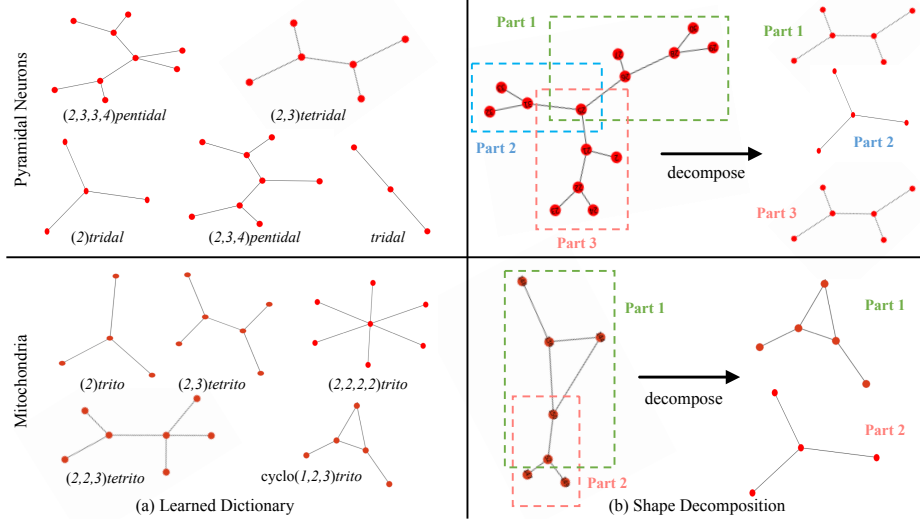


**Fig. 5.** 3D shape decomposition with topological nonmenclatures. For mitochondrion (top row) and a pyramidal neurons (bottom row), we show the learned part dictionary and (b) greedy decomposition result for an input example.

find 3D shapes which have visually similar meshes but different actual neuronal or mitochondria structures. Since the spectral embedding encodes the entire graph, it fails to find relevant shapes.

## 4.2 3D Shape Decomposition

To understand the structures of 3D shapes, we decompose topological nomenclatures into sub-graphs. To achieve this, we construct a dictionary of the proposed nomenclature embedding features. We apply  $k$ -means clustering algorithm to embedding features of junctions to generate words in the dictionary. We set  $k$  as 50 and 100 for the pyramidal neurons and mitochondria, respectively. Note that we use only the junctions since end nodes have no local structures. In the inference phase of decomposition, we perform matching between junctions in a query nomenclature and the words in the dictionary. We first find a junction with the minimum distance, and then remove it and its neighbor nodes from the query nomenclature. We iterate this process until there are no more junctions.

Figure 5 (a) visualizes dictionaries learned on the JWR-Mito300 and JWR-Pyr30 datasets. It is observable that the words in the dictionaries vary. Figure 5 (b) shows decomposition results of the proposed nomenclatures. Our proposed method decomposes the nomenclatures into sub-graphs precisely.

## 5 Conclusion

In this paper, we proposed the topological nomenclature protocol for connectomics. We demonstrated the effectiveness of the proposed nomenclature system through shape retrieval and decomposition. We will make the two datasets containing 316 mitochondria and 30 pyramidal neurons publicly available. For future work, we will apply the proposed nomenclature scheme to a large-scale dataset for understanding the diversity and similarity of biological structures.

## References

- Berger, D.R., Seung, H.S., Lichtman, J.W.: Vast: efficient manual and semi-automatic labeling of large 3d image stacks. *Frontiers in neural circuits* **12** (2018)
- Cheng, H.C., Varshney, A.: Volume segmentation using convolutional neural networks with limited training data. In: *ICIP* (2017)
- Cormen, T.H., Leiserson, C.E., Rivest, R.L., Stein, C.: *Introduction to algorithms*. MIT press (2009)
- Favre, H.A., Powell, W.H.: *Nomenclature of organic chemistry: IUPAC recommendations and preferred names 2013*. Royal Society of Chemistry (2013)
- Heller, S., McNaught, A., Stein, S., Tchekhovskoi, D., Pletnev, I.: Inchi-the worldwide chemical structure identifier standard. *J. of cheminformatics* **5**(1), 7 (2013)
- Januszewski, M., Kornfeld, J., Li, P.H., Pope, A., Blakely, T., Lindsey, L., Maitin-Shepard, J., Tyka, M., Denk, W., Jain, V.: High-precision automated reconstruction of neurons with flood-filling networks. *Nature methods* **15**(8), 605 (2018)
- Kasthuri, N., Hayworth, K.J., Berger, D.R., Schalek, R.L., Conchello, J.A., Knowles-Barley, S., Lee, D., Vázquez-Reina, A., Kaynig, V., Jones, T.R., et al.: Saturated reconstruction of a volume of neocortex. *Cell* **162**(3), 648–661 (2015)
- Kingma, D.P., Welling, M.: Auto-encoding variational bayes. In: *ICLR* (2013)
- Kipf, T.N., Welling, M.: Variational graph auto-encoders. In: *NIPS Workshop on Bayesian Deep Learning* (2016)
- McNaught, A.D., McNaught, A.D.: *Compendium of chemical terminology*, vol. 1669. Blackwell Science Oxford (1997)
- Ng, A.Y., Jordan, M.I., Weiss, Y.: On spectral clustering: Analysis and an algorithm. In: *Advances in neural information processing systems*. pp. 849–856 (2002)
- Ovsjanikov, M., Bronstein, A.M., Bronstein, M.M., Guibas, L.J.: A computer vision approach to isometry invariant shape retrieval. In: *IEEE ICCV Workshops* (2009)
- Palágyi, K.: *A sequential 3d curve-thinning algorithm based on isthmuses*. In: *Advances in Visual Computing*. Springer International Publishing (2014)
- Panico, R., Powell, W., Richer, J.C.: *A guide to IUPAC Nomenclature of Organic Compounds*. Blackwell Scientific Publications, Oxford (1993)
- Ronneberger, O., Fischer, P., Brox, T.: U-net: Convolutional networks for biomedical image segmentation. In: *MICCAI* (2015)
- Sun, J., Ovsjanikov, M., Guibas, L.: A concise and provably informative multi-scale signature based on heat diffusion. *Comput. Graph. Forum* **28** (07 2009)
- Sundar, H., Silver, D., Gagvani, N., Dickinson, S.: Skeleton based shape matching and retrieval. In: *Proceedings of the Shape Modeling International*. IEEE Computer Society (2003)
- Zheng, Z., Lauritzen, J.S., Perlman, E., Robinson, C.G., Nichols, M., Milkie, D., Torrens, O., Price, J., Fisher, C.B., Sharifi, N., et al.: A complete electron microscopy volume of the brain of adult drosophila melanogaster. *Cell* **174**(3) (2018)



Supplementary Materials on:  
**A Topological Nomenclature for 3D Shape Analysis in  
Connectomics**

Abhimanyu Talwar, Zudi Lin, Donglai Wei, Yuesong Wu, Bowen Zheng,  
Jinglin Zhao, Won-Dong Jang, Xueying Wang, Jeff W. Lichtman, and  
Hanspeter Pfister

Harvard University, Cambridge, MA 02138, USA

**Cosine Similarity of Laplacian Eigenvalues for Mitochondria: Ground Truth vs. Reduced Graph**

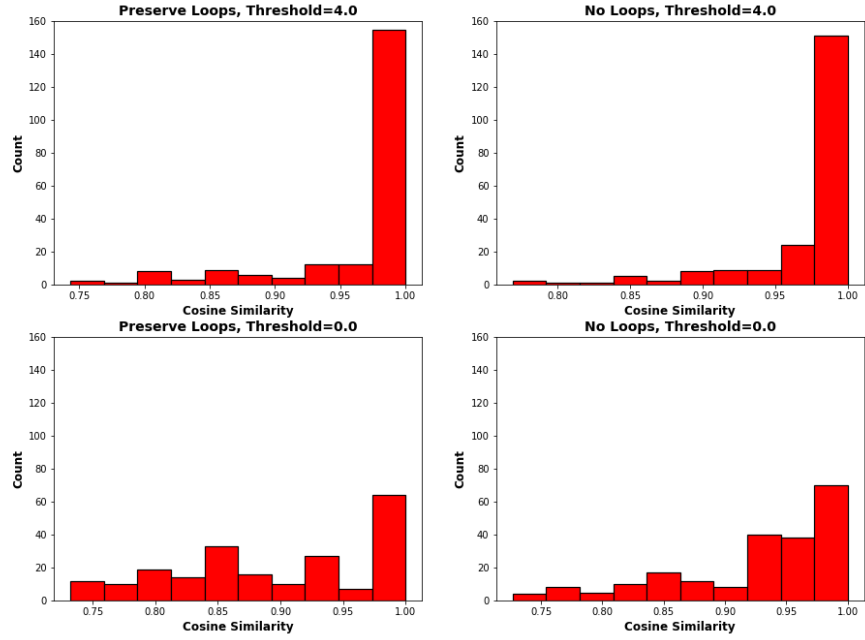


**Fig. 1.** Ablation studies for the threshold  $\tau$  in Section 2.1 on 213 mitochondria: we compare ground truth graphs provided by neuroscientists and our reduced graph representation by measuring cosine similarities between Laplacian eigenvalues of them. “Preserve Loops” and “No Loops” indicate whether to preserve loops presented in the skeleton graph or ignore them, respectively. We observe that the choice of threshold for collapsing small edges is crucial, as it shows higher cosine similarities when we use a threshold value of 4.0 versus the setting without thresholding. Preservation of loops seems to have a small impact on overall performance, but it is still important for preserving the topology of cyclic mitochondria even if they rarely appear in neurons.

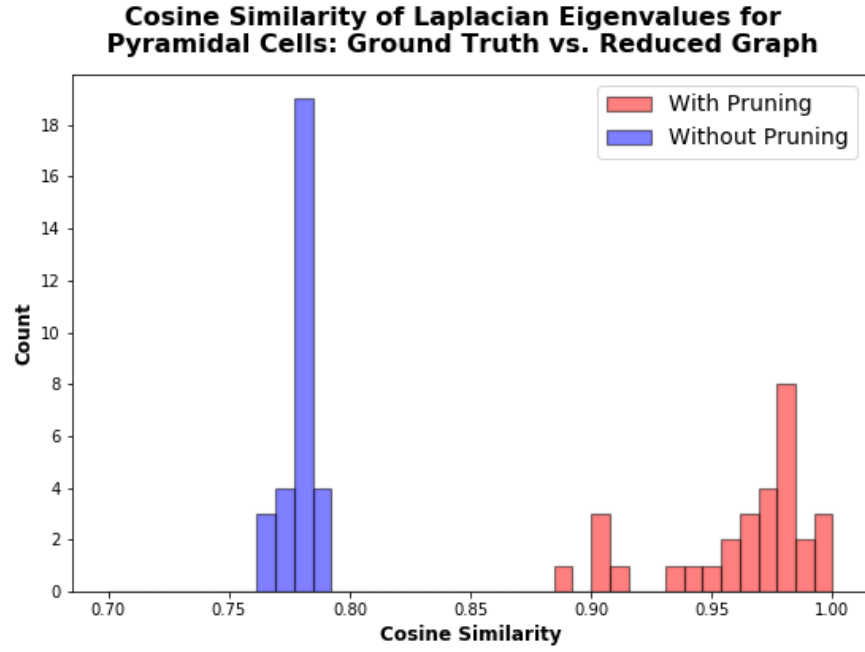


**Fig. 2.** Ablation studies for 25 pyramidal cells: we compare cosine similarities between Laplacian eigenvalues of ground truth graphs drew by neuroscientists and our reduced graphs with and without pruning. Pruning is a process controlling the minimal length of branches. We observe that reduced graphs extracted with post-pruning lead to higher cosine similarities than in the graph without pruning. It shows our representations capture essential topology without producing disturbing artifacts.

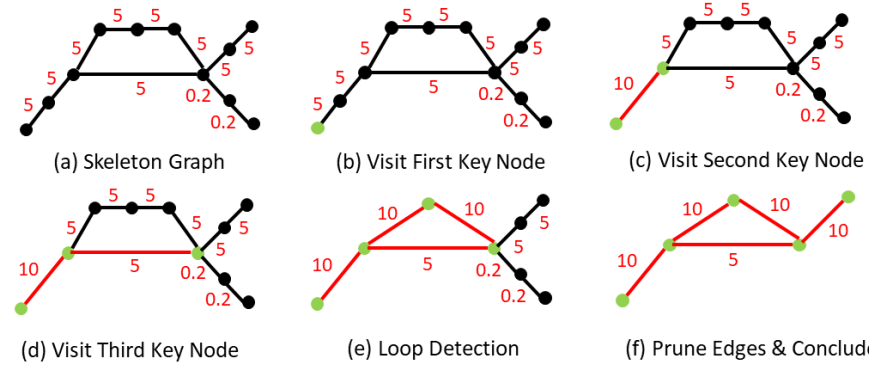


**Fig. 3.** Illustration of our algorithm for extracting reduced graph from a naive skeleton graph. We have modified the breadth-first search (BFS) traversal to consider only key nodes in the graph. Unlike BFS which results in a tree, our traversal preserves loops within the graph to maintain the cyclic topology of some mitochondria and pyramidal neurons that form loops.

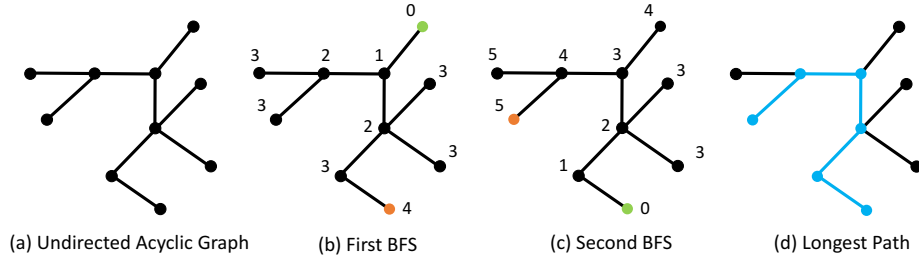


**Fig. 4.** Illustration of extracting the longest path for the nomenclature assignment of undirected acyclic graphs (UAG) (Sec. 2.2). Although the longest-path problem in an arbitrary graph is *NP*-complete, the problem can be efficiently solved by running the breadth-first search (BFS) algorithm twice for UAGs. The first pass starts from an arbitrary leaf point (b), while the second pass starts from the farthest point found in the first round (c).